Quantifying uncertainties in simulating wheat yields under climate change

S. Asseng, F. Ewert, C. Rosenzweig, J.W. Jones, J.L. Hatfield, A. Ruane, K.J. Boote, P. Thorburn, R.P. Rötter, D. Cammarano, N. Brisson, B. Basso, P. Martre, P.K. Aggarwal, C. Angulo, P. Bertuzzi, C. Biernath, A.J. Challinor, J. Doltra, S. Gayler, R. Goldberg, R. Grant, L. Heng, J. Hooker, L.A. Hunt, J. Ingwersen, R.C. Izaurralde, K.C. Kersebaum, C. Müller, S. Naresh Kumar, C. Nendel, G. O'Leary, J.E. Olesen, T. M. Osborne, T. Palosuo, E. Priesack, D. Ripoche, M.A. Semenov, I. Shcherbak, P. Steduto, C. Stöckle, P. Stratonovitch, T. Streck, I. Supit, F. Tao, M. Travasso, K. Waha, D. Wallach, J.W. White, J.R. Williams and J. Wolf

Supplementary Information

Supplementary Materials and methods

Partially and fully calibrated simulation experiments (Fig. 1 and 2) with observed field experimental data

Twenty-seven different wheat crop simulation models were used by individual modeling groups (in most cases by the model developers) (Supplementary Table S1) for a model intercomparison. The models varied in complexity and functionality (Supplementary Table S2). Six models did not simulate nitrogen (N) dynamics (Supplementary Table S2). Simulations were carried out for single treatments of experiments at four contrasting locations, which were The Netherlands (Wageningen[1]), Argentina (Balcarce[2]), India (New Delhi[3]), and Australia (Wongan Hills[4]) (Supplementary Table S3) representing a very wide range of growing conditions of wheat. Crop management treatments were chosen to be representative for each region (Supplementary Table S3).

Supplementary Table S1. Crop models (27) used in AgMIP Wheat study.

Model (version)	Reference	Documentation
APSIM-Nwheat (V.1.55)	[4-6]	http://www.apsim.info
APSIM (V.7.3)	[6]	http://www.apsim.info/Wiki/
AquaCrop (V.3.1+)	[7]	http://www.fao.org/nr/water/aquacrop.html
CropSyst (V.3.04.08)	[8]	http://www.bsyse.wsu.edu/CS_Suite/CropSyst/index.html
DSSAT- CERES (V.4.0.1.0)	[9, 10, 11]	http://www.icasa.net/dssat/
DSSAT-CROPSIM (V4.5.1.013)	[10, 12]	http://www.icasa.net/dssat/

Ecosys	[13]	https://portal.ales.ualberta.ca/ecosys/
EPIC wheat (V1102)	[14-16]	http://epicapex.brc.tamus.edu/
Expert-N (V3.0.10) - CERES (V2.0)	[17-20]	http://www.helmholtz-muenchen.de/en/iboe/expertn/
Expert-N (V3.0.10) – GECROS (V1.0)	[19, 20]	http://www.helmholtz-muenchen.de/en/iboe/expertn/
Expert-N (V3.0.10) – SPASS (2.0)	[17, 19-22]	http://www.helmholtz-muenchen.de/en/iboe/expertn/
Expert-N (V3.0.10) - SUCROS (V2)	[17, 19, 20, 23]	http://www.helmholtz-muenchen.de/en/iboe/expertn/
FASSET (V.2.0)	[24, 25]	http://www.fasset.dk
GLAM-wheat (V.2)	[26, 27]	http://see-web-01.leeds.ac.uk/research/icas/climate_change/glam/download_glam.html
HERMES (V.4.26)	[28, 29]	http://www.zalf.de/en/forschung/institute/lsa/forschung/oekomod/hermes
InfoCrop (V.1)	[30]	http://www.iari.res.in
LINTUL-4 (V.1)	[31, 32]	http://models.pps.wur.nl/models
LINTUL-FAST (V.1)	[33]	Request from frank.ewert@uni-bonn.de
LPJmL (V3.2)	[34-39]	http://www.pik-potsdam.de/research/projects/lpjweb
MCWLA-Wheat (V.2.0)	[40-42 43]	Request from taofl@igsnrr.ac.cn
MONICA (V.1.0)	[44]	http://monica.agrosystem-models.com
O'Leary-model (V.7)	[45-48]	Request from gjoleary@yahoo.com
SALUS (V.1.0)	[49, 50]	http://www.salusmodel.net
Sirius (V2010)	[51-54]	http://www.rothamsted.ac.uk/mas-models/sirius.php
SiriusQuality (V.2.0)	[55-57]	Request from pierre.martre@clermont.inra.fr
STICS (V.1.1)	[58, 59]	http://www.avignon.inra.fr/agroclim_stics_eng/
WOFOST (V.7.1)	[60]	http://www.wofost.wur.nl

Supplementary Table S2. Modeling approaches of 27 wheat simulation models used in AgMIP wheat study.

Model	Leaf area / light interception [a]	Light utilization [b]	Yield formation [c]	Phenology [d]	Root distribution over depth [e]	Environmental constraints involved [f]	Type of water stress [g]	Type of heat stress [h]	Water dynamics [i]	Evapotranspiration [j]	Soil CN-model [k]	Process modified by elevated CO_2 [l]	No. cultivar parameters	Climate input variables [m]	Model relative [n]	Model type [o]
APSIM-Nwheat	S	RUE	Prt	T/DL/V	EXP	W/N/A	S	V	C	PT	CN/P(3)/B	RUE/TE	7	R/Tx/Tn/Rd	C	P
APSIM-wheat	S	RUE	Prt/Gn/B	T/DL/V/O	O	W/N/A	E	-	C/R	**PT**/PM	CN/P(3)/B	RUE/TE/CLN	7	R/Tx/Tn/Rd/e/W	C	P
AquaCrop	S	TE	HI/B	T/DL/V/O	EXP	W/N/H	E/S	V/R	C	PM	none	TE	2	R/Tx/ETo	none	P
CropSyst	S	TE/RUE	HI/B	T/DL/V	EXP	W/N/H	E	R	C/R	PM	N/P(4)	TE/RUE	16	R/Tx/Tn/Rd/RH/W	none	P
DSSAT-CERES	S	RUE	B/Gn	T/DL/V	EXP	W/N	E/S	-	C	PT	CN/P(4)/B	RUE/TE	7	R/Tx/Tn/Rd/RH/W	C	P
DSSAT-CROPSIM	S	RUE	Prt	T/DL/V	LIN	W/N	E/S	V	C	PT	CN/P(4)/B	RUE/TE	21	R/Tx/Tn/Rd/	none	p
Ecosys	D	P-R	Gn-Prt	T/DL/V/O	Call	W/N/A/H	E/S	V/R	R	EB	P30/B5	F	2	R/Tx/Tn/Td/Rd/W	none	P
EPIC wheat	S	RUE	HI	T/V	EXP	W/N/H	E	V	C	P/**PM**/PT/HAR	N/P(5)/B	RUE/TE/GY	16	R/Tx/Tn/Rd/RH/W	E	P/G
Expert-N – CERES	S	RUE	B/Gn	T/DL/V	EXP	W/N	E/S	-	R	PM	CN/P(3)/B	RUE	7	R/Tx/Tn/Rd/RH/W	C	P
Expert-N – GECROS	D	P-R/TE	Gn/Prt	T/DL/V	EXP	W/N	E/S	-	R	PM	CN/P(3)/B	RUE/TE	10	R/Tx/Tn/Rd/RH/W	S	P
Expert-N – SPASS	D	P-R	Gn/Prt	T/DL/V	EXP	W/N	E/S	-	R	PM	CN/P(3)/B	RUE	5	R/Tx/Tn/Rd/RH/W	C/S	P
Expert-N – SUCROS	D	P-R	Prt	T	EXP	W/N	E/S	-	R	PM	CN/P(3)/B	RUE	2	R/Tx/Tn/Rd/RH/W	S	P
FASSET	D	RUE	HI/B	T/DL	EXP	W/N	E/S	-	C	MAK	CN/P(6)/B	RUE	14	R/Tx/Tn/Rd	none	P
GLAM-Wheat	S	RUE/TE	B/HI	T/DL/V	LIN	W/H	E	R	C	PT	none	RUE/TE	22	R/Tx/Tn/Td/Ta/e	none	G
HERMES	D	P-R	Prt	T/DL/V/O	EXP	W/N/A	E/S	-	C	**PM**/TW/PT	N/P(2)	RUE/F	6	R/Tx/Tn/Rd/e/RH/W	S/C	P
InfoCrop	D	RUE	Prt/Gn	T/DL	EXP	W/N/H	E	V/R	C	**PM**/PT	CN/P(2)/B	RUE/TE	10	R/Tx/Tn/Rd/W/e	S	P
LINTUL-4	D	RUE	Prt/B	T/DL	LIN	W/N/A	E	-	C	P	N/P(0)*	RUE/TE	4	R/Tx/Tn/Rd/e/W	L	P
LINTUL-FAST	D	RUE	Prt	T/DL/V	EXP	W	E	-	C	PM	CN/P(3)	RUE/TE	4	R/Tx/Tn/Rd/RH	L	P

LPJmL	S	P-R	HI_mws/B	T/V	EXP	W	E	-	C	PT	none	F	3	R/Ta/Rd/Cl	E	G
MCWLA-Wheat	S	P-R	HI/B	T/DL/V	EXP	W/H	E	V/ R	R	PM	none	F	7	R/Tx/Tn/Rd/e/W	none	G
MONICA	S	RUE	Prt	T/DL/V/O	EXP	W/N/A/H	E	V	C	PM	CN/P(6)/B	F	15	R/Tx/Tn/Rd/RH/W	H	P
O'Leary-model	S	TE	Gn/Prt	T/DL	SIG	W/N/H	E/S	V	C	P	N/P(3)/B	TE	18	R/Tx/Tn/Rd/RH/W	none	P
SALUS	S	RUE	Prt/HI	T/DL/V	EXP	W/N/H	E	V	C	PT	CN/P(3)/B(2)	RUE	18	R/Tx/Tn/Rd	C	P
Sirius	D	RUE	B/Prt	T/DL/V	EXP	W/N	E	-	C	P/**PT**	N/P(2)	RUE	14	R/Tx/Tn/Rd/e/W	none	P
SiriusQuality	D	RUE	B/Prt	T/DL/V	EXP	W/N	S	-	C	**P**/PT	N/P(2)	RUE	14	R/Tx/Tn/Rd/e/W	I	P
STICS	D	RUE	Gn/B	T/DL/V/O	SIG	W/N/H	E/S	V/R	C	P/PT/ **SW**	N/P(3)/B	RUE/TE	15	R/Tx/Tn/Rd/e/W	C	P
WOFOST	D	P-R	Prt/B	T/DL	LIN	W/N*	E/S	-	C	P	P(1)	RUE/TE	3	R/Tx/Tn/Rd/e/W	S	G

[a] S, simple approach (e.g. LAI); D, detailed approach (e.g. canopy layers).
[b] RUE, radiation use efficiency approach; P-R, gross photosynthesis – respiration; TE, transpiration efficiency biomass growth.
[c] HI, fixed harvest index; B, total (above-ground) biomass; Gn, number of grains; Prt, partitioning during reproductive stages; HI_mw, harvest index modified by water stress.
[d] T, temperature; DL, photoperiod (day length); V, vernalization; O, other water/nutrient stress effects considered.
[e] LIN, linear, EXP, exponential, SIG, sigmoidal, Call, carbon allocation; O, other approaches.
[f] W, water limitation; N, N limitation; A, aeration deficit stress; H, heat stress.
[g] E, actual to potential evapotranspiration ratio; S, soil available water in root zone.
[h] V, vegetative organ (source); R, reproductive organ (sink).
[i] C, capacity approach; R, Richards approach.
[j] P, Penman; PM, Penman-Monteith; PT, Priestley –Taylor; TW, Turc-Wendling; MAK, Makkink; HAR, Hargreaves; SW, Shuttleworth and Wallace (resistive model); EB, energy balance ("bold" indicates approached used during the study).
[k] CN, CN model; N, N model; P(x), x number of organic matter pools; B, microbial biomass pool.
[l] RUE, radiation use efficiency; TE, transpiration efficiency; GY, grain yield; CLN, critical leaf N concentration; F, Farquhar model.
[m] Cl, cloudiness; R, precipitation; Tx, maximum daily temperature; Tn, minimum daily temperature; Ta, average daily temperature; Td, dew point temperature; Rd, radiation; e, vapor pressure; RH, relative humidity; W, wind speed.
[n] C, CERES; L, LINTUL; E, EPIC; S, SUCROS; I, Sirius; H, HERMES.
[o] P, point model; G, global or regional model (regarding the main purpose of model).
[*] N-limited yields can be calculated for given soil N supply and N fertilizer applied, but model has no N simulation routines.

Supplementary Table S3. Field experiments, crop management and climate characteristics for baseline and a late century, high emission scenario (A2) used in partially calibrated and calibrated simulation experiments.

	Experiment			
	A[a]	**B**[b]	**C**[c]	**D**[d]
Location	Wageningen	Balcarce	New Delhi	Wongan Hills
Country	The Netherlands	Argentina	India	Australia
Latitude	51.97	-37.5	28.38	-30.89
Longitude	5.63	-58.3	77.12	116.72
Environment	high-yielding long-season	high/medium-yielding medium-season	irrigated short-season	low-yielding rain-fed short-season
Average growing season	November-July	June-December	November-April	May-December
Soils				
Soil type	Silty clay loam	Clay loam	Sandy loam	Loamy sand
Maximum Root depth (cm)	200	130	160	210
PAWC[†] (mm to maximum rooting depth)	354	205	121	125
Crop management				
Cultivar	Arminda	Oasis	HD 2009	Gamenya
Sowing date (DOY[‡])	294	223	328	164
Total applied N fertilizer (kg N/ha)	160	120	120	50
Total irrigation (mm)	0	0	383	0
Phenology				
Anthesis (DOY)	178	328	49	275
Maturity (DOY)	213	363	93	321
Experimental year	1982/83	1992	1984/85	1984
Mean growing season temperature	8.8 °C	13.7 °C	17.3 °C	14.0 °C
Mean growing season precipitation	595 mm	336 mm	383 mm[*]	164 mm
Baseline				
Mean growing season temperature	8.5 °C	12.0 °C	18.9 °C	16.2 °C
Mean growing season precipitation	716 mm	395 mm	467 mm*	246 mm
Climate change scenario[**]				
GCM scenario examined	ukmo_hadcm3	ncar_ccsm3.0	mpi_echam5	csiro_mk3.0
Mean growing season	11.4 °C	14.2 °C	23.6 °C	18.7 °C

temperature				
Mean growing season precipitation	690 mm	432 mm	583 mm*	164 mm

[†]Plant Available Water Content (PAWC, mm)

[‡]Day of Year (DOY)

[*] Includes 383 mm of irrigation each year

[**]A2 emission scenario from UKMO HadCM3 simulations, with 734 ppm CO_2 at 2085 was assumed in the climate model and the crop model simulations.

[a] Source: [1]

[b] Source: [2]

[c] Source: [3]

[d] Source: [4]

Sensitivity analysis with 30-years of climate data

In addition to simulations of the single-year experiments, simulations were carried out with long-term measured daily climate data (solar radiation, maximum and minimum temperature, precipitation, surface wind, dew point temperature, relative humidity, and vapor pressure) using measured soil characteristics, measured initial soil water and soil N contents, crop management, measured anthesis and maturity dates from the single-year-experiments. For the baseline, daily climate data for the period 1980-2010 were used for all locations (31 years of climate data are required to simulate 30 years of yields in The Netherlands and India). For the location in India, solar radiation was obtained from the NASA/POWER dataset that extends back to 1983 (http://power.larc.nasa.gov). Missing data for 1980 to 1983 were filled in using the Weatherman tool included in DSSAT 4.5[61]. In addition, 2-meter wind speed (m/s), dew point temperature (ºC), vapor pressure (hPa), and relative humidity (%) were estimated for each location from the NASA Modern Era Retrospective-Analysis for Research and Applications (MERRA[62]). For the location in The Netherlands, measured wind speed and vapor pressure were available.

Each of the 27 wheat models was used to simulate the field experiments in two separate steps, 1) with limited in-season information from the experiments being made available to the modelers (partial calibration or 'blind' simulations), and 2) all available information being made available to the modelers (full calibration). Simulations with partially calibrated models were included to allow a more objective model assessment[63]. For the partial calibration or 'blind model test',

modelers had no access to measurements of grain yield, biomass, and crop water and N dynamics, receiving information only on soil characteristics, initial soil-water conditions, daily weather data, crop management, and flowering and maturity dates. For full calibration, modelers had access to all available measurements, including within-season and final biomass, water and N uptake, soil water and soil N, grain yield and yield components.

Note, some of these data may have been used, as part of a larger data set (NL and AU), for past calibration of some of the models. Furthermore, the organization of the project was such that one modeling group had access at all times to detailed data from all four sites, one group had access to NL and AU and one group had access to NL and did know the measurements beforehand. However, they did not change the model or parameters for the blind test as a consequence.

The annual simulation outputs included: grain yield (t ha^{-1}); above-ground biomass at anthesis (kg ha^{-1}); above-ground biomass at maturity (kg ha^{-1}); maximum leaf area index (LAI, m^2 m^{-2}); anthesis date (DOY); maturity date (DOY); cumulative N leached (kg N ha^{-1}); cumulative water loss (mm); total above-ground N at anthesis (kg N ha^{-1}); total above-ground N at maturity (kg N ha^{-1}); grain N (kg N ha^{-1}); grains per square meter (# m^{-2}); cumulative ET (mm); cumulative N mineralization (kg N ha^{-1}); cumulative N volatilization (kg N ha^{-1}); cumulative N immobilization (kg N ha^{-1}); cumulative N denitrification (kg N ha^{-1}); plant available soil water to maximum rooting depth (mm); soil mineral N to maximum rooting depth (kg N ha^{-1}).

Data analysis (Fig. 1, 2 and 3a-d)

The root mean square error (RMSE) between observed and simulated yield is calculated as:

$$\text{RMSE} = \sqrt{\frac{1}{n}\sum_{i=1}(y_i - \hat{y}_i)^2} \qquad (1)$$

where y_i are the measurements, $\hat{y}_i$the simulations, and *n* is the number of comparisons.

For the analysis in Fig. 1c, +/- 13.5% was used as the measurement uncertainty. That is the mean coefficient of variation (CV) for more than 300 wheat field experiments reported in Taylor et al. [64]. For Fig. 2a-d, we define model response to changed climate as:

$$x_k = \bar{y}_{future,k} - \bar{y}_{baseline,k} \qquad (2)$$

where x_k is predicted yield change according to model *k*, $\bar{y}_{future,k}$ is yield averaged over the 30 years of future climate according to model *k* and $\bar{y}_{baseline,k}$ is yield averaged over the 30 years of baseline climate according to model *k*. The coefficient of variation (CV%) of *x* represents the variation between models, calculated as:

$$CV\% = \frac{\sigma}{\bar{x}} * 100 \qquad (3)$$

where σ is the standard deviation of the yield changes (x) values and $\bar{x}$ is their average. Coefficients of variation were calculated separately for the partially calibrated models, the fully calibrated models, the 50% of fully calibrated models that have the smallest RMSE averaged over all locations and finally for each location the 50% of fully calibrated models (14 of 27) with the smallest RMSE for each particular location.

The relative grain yield change in Fig. 3a-d was calculated as:

$$r_k = \frac{\bar{y}_{future,k} - \bar{y}_{baseline,k}}{\bar{y}_{baseline,k}} * 100 \qquad (4)$$

The box and whisker plots show the distribution of responses from the wheat models. The vertical line in each box represents the median response, the box delimits the 25th to 75th percentiles, and the whiskers extend from the 10th to the 90th percentile.

Variation in model predictions of the effect of climate change in relation to calibration, soil and crop management (Fig. 2)

For Fig. 2, the 30-year base line climate assumes a CO_2 concentration of 360 ppm CO_2 (mean of 1995). The 30-year climate change scenario, an A2 emission scenario for 2070-2099 with 734 ppm CO2 at 2085, was drawn from the single GCM that best represented the seasonal temperature and precipitation changes from the wider ensemble of GCMs at the given location (Supplementary Table S3). This emission scenario (A2) and future time period (2070-2099) was selected as one with extreme expected changes in temperature and precipitation over the next 100 years for a sensitivity analysis. This ensured that the largest projected changes in climate are included in the model sensitivity analysis. The same local soil and crop management (except N and irrigation) was used for the baseline and sensitivity scenario. The crop management represents current practice at the selected locations, representative for the region of the location. Simulations were reset each year to the measured soil water and soil N contents from the field experiments before sowing to avoid carry-over effects. Dates for in-season crop management, N fertilizer (The Netherlands, India) and irrigation (India), were adjusted for phenology changes due to temperature changes in the sensitivity scenarios. An average application date was applied to each of the 30 years for each of the baseline, and sensitivity scenarios according to the mean temperature changes.

To analyze the impact of different soils, soil properties were manipulated by creating a +/-20%[65, 66] water-holding capacity at each location by changing the drained upper limit in each soil layer accordingly. To analyze the impact of different N-fertilizer management, N-fertilizer applications were varied by adjusting the N applications by +/-50% relative to the local crop management practice. To analyze the impact of sowing dates, the sowing dates were shifted 20 days earlier and 20 days later than the locally practiced sowing date.

Variation in model predictions (Fig. 3a-d)

The sensitivity analysis of Fig. 3 was carried out with 26 of the 27 wheat models (one modeling group was not able to carry out the sensitivity analysis), using the fully calibrated models. The relative yield changes are calculated as in eq. (4). The future weather scenarios use the baseline

weather with temperature changes of -3°, 0°C, +3°C, +6°C or +9°C and CO_2 concentrations in 90 ppm increments from 360 ppm to 720 ppm (see Supplementary Table S4). Temperature changes were added to daily minimum and maximum temperature as used in the models. In addition to the scenarios presented in Fig. 2, scenarios with changes in N fertilization (Supplementary Table S4) and some specific combinations of changes in future climate and crop management (Supplementary Table S5) were tested.

Supplementary Table S4. Variable combinations altered in the sensitivity experiment[†]. All temperature by CO_2 combinations were simulated. +/-N was applied to all CO_2 changes, but not in combination with temperature.

Variable	**Change**				
Baseline weather with Temperature[‡]	-3°C	0° C	+3°C	+6°C	+9°C
Baseline weather with CO_2 concentration	360 ppm	450 ppm	540 ppm	630 ppm	720 ppm
Baseline weather with N[*]	100%	50%	150%		

[†] Carried out with 26 crop models (one modeling group was not able to participate in this analysis) for the four locations with 30 years. Changes were applied to 30-year baseline weather data (1981-2010).

[‡] Note, T_{max} and T_{min} were changed simultaneously for each day and all the temperatures are offsets from baseline temperature.

* Six crop models do not simulate N dynamics.

Supplementary Table S5. Climate-by-crop-management experiments[†].

Description
Baseline (360 ppm) + 7 days of T_{max}=35 ^{o}C start at measured anthesis date[x]
Baseline (360 ppm) - 20 days in sowing date
Baseline (360 ppm) + 20 days in sowing date
Baseline (360 ppm) - 20% PAW[‡] of soil
Baseline (360 ppm) + 20% PAW[‡] of soil
A2-End-of-Century scenario** 734 ppm - 20 days in sowing date
A2- End-of-Century scenario** 734 ppm + 20 days in sowing date
A2- End-of-Century scenario** 734 ppm 50% N fertilizer[*]
A2- End-of-Century scenario** 734 ppm 150% N fertilizer[*]
A2- End-of-Century scenario** 734 ppm - 20% PAW of soil
A2- End-of-Century scenario** 734 ppm + 20% PAW of soil

[†]Carried out with 26 crop models (one modeling group was not able to participate in this analysis) for the four locations with 30 years. Changes were applied to 30-year baseline weather data (1981-2010).

[x]Baseline temperatures were modified by including a maximum temperature of 35°C for 7 days starting at measured anthesis date for each location. If baseline temperatures exceeded 35°C, values were not adjusted.

[‡]PAW - Plant available water holding capacity of a soil. PAW was reduced or increased by 20% by changing the drain upper limit of the soil.

*Six models do not include N dynamics.

**Modified baseline climate series for each location according to GCM scenario listed in Table S3 to represent A2 End-of-Century (2070-2099) scenarios; 734 ppm CO_2 represents 2085 concentration from A2 scenario.

Observed impact of elevated CO_2 and temperature (Fig. 3e)

Fig. 3e in the main paper is based on the following data: Several FACE experiments in the USA, Germany and China have reported an 8 to 26 % grain yield increase with elevated atmospheric CO_2 concentrations of 550 ppm compared with 360 ppm[67-72]. Similarly, an average 3 to 10% wheat grain yield decline per 1^{o}C increase in mean temperature has been reported across several experiments[67, 73], though there is some evidence that the impact of temperature change on grain yield might be non-linear[74]. Acknowledging this, but for simplicity here, the reported impacts

were linearly extrapolated in Fig. 3e to +3°C to allow for a general comparison with the simulation results in Fig. 3a-d.

Calculation of required number of models to reduce uncertainty (Fig. 4a)

Figure 4a is based on a sensitivity analysis with five temperature levels and five CO_2 concentrations at 100% N (Supplementary Table S4). We evaluated how variable the results would be if the number of models varied from m=1 to m=26 (one of the 27 models was not used in the sensitivity analysis). For each value of m, and for each site, we drew at random 260 combinations of model results (10 times the number of models, each representing a model) and calculated CV%. A typical result is shown in Supplementary Figure S1 for one of the locations, India. Such analysis was carried out for each location. The smallest m such that CV% < 13.5% (which is the experimental variation reported by Taylor et al.[64]) is the number of models reported. The average value of m across the four study locations is presented in Fig. 4a.

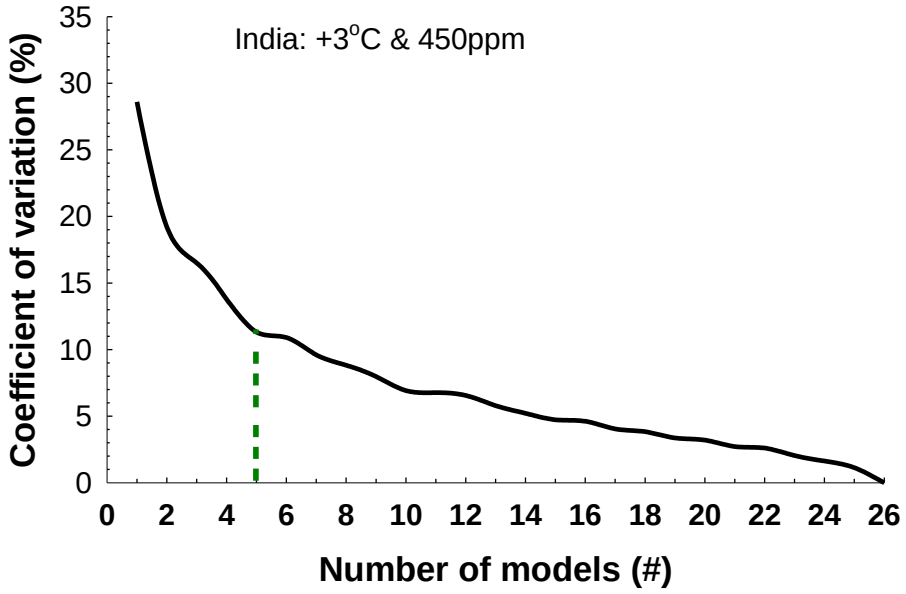

Supplementary Figure | S1. Illustration of calculated coefficient of variation (CV%) of simulated yield responses to a combination of temperature and CO_2 changes (+3 °C and 450 ppm) as a function of the number of average model responses randomly selected 260 times from the model results (calibrated models) for India. Vertical green line indicates number of models chosen in this case, i.e. the smallest number of models below the 13.5 CV% after Taylor et al.[64].

Comparing uncertainties of crop and General Circulation Models (Fig. 4b)

A scenario representing a A2 emission scenario for the 2040-2069 period (also referred to as 2050s, Mid- Century, 556 ppm of CO_2) from the ensemble of 16 General Circulation Models (GCM) (Supplementary Table S6) was used by 26 wheat models (one modeling group was not able to carry out this analysis). 30-year mean climatologies from each GCM were calculated for each month and the Mid-Century grid boxes corresponding to the four experimental locations were compared to the same grid box in the baseline period (1980-2009). The resulting monthly changes (aggregated to growing season means in Supplementary Table S7, but applied here on a monthly basis) were then imposed on the observed 30-year daily baseline climate series baselines following the so-called "delta change approach"[75].

Each crop model simulated each of the 16 GCM scenarios. The 30-year mean absolute impacts of the scenarios were calculated (30-year scenario mean minus 30-year baseline mean). Standard deviations were calculated for the absolute yield impacts separately across crop models and across the GCM's by using the model results from the 10^{th} percentile to the 90^{th} percentile of simulations based on multi-models (i.e. considering the $0\text{-}10^{th}$ and $90\text{-}100^{th}$ percentiles as outliers, consistent with the whisker plots used here). Standard deviations were used to calculate the coefficients of variation (CV%, equation 3) by using the observed grain yields from each location (supplied in Figure 4b) as basis for the calculation of CV to be directly comparable with observed data shown in Figure 1.

Supplementary Table S6: Sixteen General Circulation Models (GCM) models from CMIP3 General Circulation Models analyzed[76] used for climate changes scenarios.

GCM scenario	GCM	GCM source
A	bccr_bcm2.0	Bjerknes Centre for Climate Research, Norway
B	cccma_cgcm3.1(T63)	Canadian Centre for Climate Modeling and Analysis, Canada
C	cnrm_cm3	CERFACS, Center National Weather Research , METEO-FRANCE, France

D	csiro_mk3.0	CSIRO Atmospheric Research, Australia
E	gfdl_cm2.0	Geophysical Fluid Dynamics Laboratory, USA
F	gfdl_cm2.1	Geophysical Fluid Dynamics Laboratory, USA
G	giss_modelE_r	NASA Goddard Institute for Space Studies, USA
H	Inmcm3.0	Institute for Numerical Mathematics, Russia
I	ipsl_cm4	Institute Pierre Simon Laplace, France
J	miroc3.2 (medium resolution)	Center for Climate System Research; National Institute for Environmental Studies; Frontier Research Center for Global Change, Japan
K	miub_echo_g	Meteorological Institute of the University of Bonn, Germany
L	mpi_echam5	Max Planck Institute for Meteorology, Germany
M	mri_cgcm2.3.2a	Meteorological Research Institute, Japan
N	ncar_ccsm3.0	National Center for Atmospheric Research, USA
O	ncar_pcm1	National Center for Atmospheric Research, USA
P	ukmo_hadcm3	Hadley Centre for Climate Prediction, Met Office, UK

Supplementary Table S7: Projected change in mean growing-season temperature and percentage change in mean growing-season precipitation at each location for A2-2040-2069 (Mid- Century) scenarios from 16 GCMs.

Location	**Wageningen**	**Balcarce**	**New Delhi**	**Wongan Hills**
Country	**The Netherlands**	**Argentina**	**India**	**Australia**
GCM scenario	Change in mean growing season† temperature (°C)			
A	1.56	1.26	1.58	1.24
B	1.39	1.01	2.63	1.85
C	1.67	1.29	2.12	1.56
D	1.33	1.01	1.62	1.51
E	1.52	1.27	3.00	1.55

F	1.12	1.01	2.22	1.50
G	1.84	0.84	2.13	1.88
H	1.44	1.37	2.95	1.34
I	2.14	1.33	2.42	1.84
J	1.96	1.33	2.17	1.51
K	1.20	1.13	1.73	1.53
L	1.46	0.77	2.20	1.54
M	1.28	1.19	1.65	1.30
N	1.96	1.33	2.22	2.23
O	1.06	1.00	1.53	1.03
P	1.22	1.60	2.42	1.84

GCM scenario	Change in mean growing season[†] precipitation (%)			
A	8.7	10.4	-18.7	-14.1
B	6.3	0.4	-9.1	-23.3
C	2.3	1.7	-31.3	-21.5
D	16.8	12.4	6.5	-24.5
E	1.8	-8.3	-40.1	-29.2
F	2.2	-7.2	46.2	-24.2
G	-1.1	2.1	-2.3	-15.5
H	12.2	0.9	10.4	-19.1
I	-7.8	-14.3	-0.2	-21.4
J	2.5	-2.4	-6.7	-8.8
K	6.5	-5.1	27.7	-19.0
L	-1.4	-3.5	13.7	-22.8
M	4.4	-2.8	57.2	5.9
N	0.9	-4.9	12.0	-7.5
O	4.6	-0.7	-12.2	-12.9
P	-3.8	3.3	68.1	15.6

[†]Current growing season length. See Supplementary Table S3 for location specific growing season periods.

Supplementary Results

Precipitation impact

The simulated 30-year baseline yields were used to analyze the impact of growing-season precipitation changes on simulated yields. After sorting years according to mean seasonal temperature, yields from the mid-temperature tercile of the 30-year baselines for each location (except India which received irrigation) were selected to minimize a temperature effect, and compared with the yield from the year with the mean precipitation of this tercile. Years with about +10 and +25% higher growing-season precipitation and years with -10 and -25% less growing-season precipitation than the median of the mid-tercile were selected to calculate yield impacts from precipitation differences (i.e. difference in yield from year with +10, +25% higher precipitation, -10 and -25% less growing-season precipitation and the yield of the median precipitation year of the mid-temperature tercile. Growing-season precipitation differences had an impact on simulated yield but showed little impact on the variation in simulated yield change due to precipitation changes (Supplementary Fig. S2).

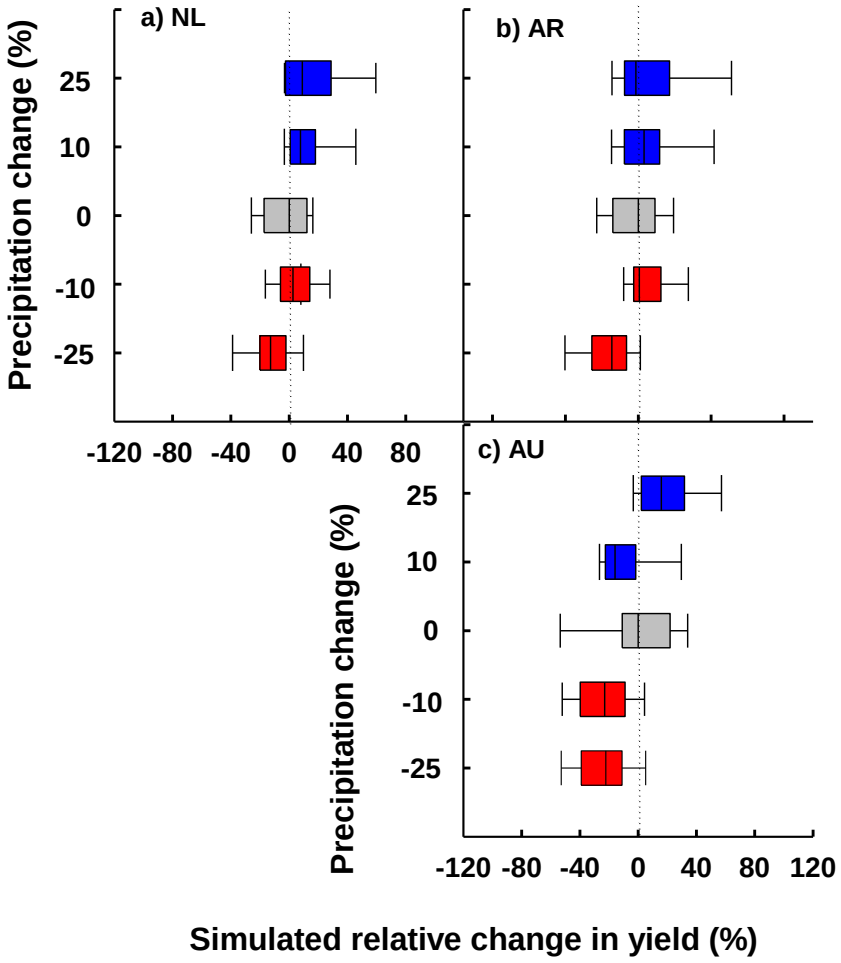

Supplementary Fig. S2. Simulated relative grain yield difference (change) for an increase (+10 and +25%) and a decrease (-10, -25%) in growing-season precipitation for the rain-fed sites a) The Netherlands (NL), b) Argentina (AR) and c) Australia (AU). For each box plot, vertical lines represent, from left to right, the 10th percentile, 25th percentile, median, 75th percentile and 90th percentile of simulations based on multi-models.

High temperature impact

Increased temperatures had an impact on simulated anthesis and maturity dates (Supplementary Fig. S3), which in turn affect simulated growth and grain yields.

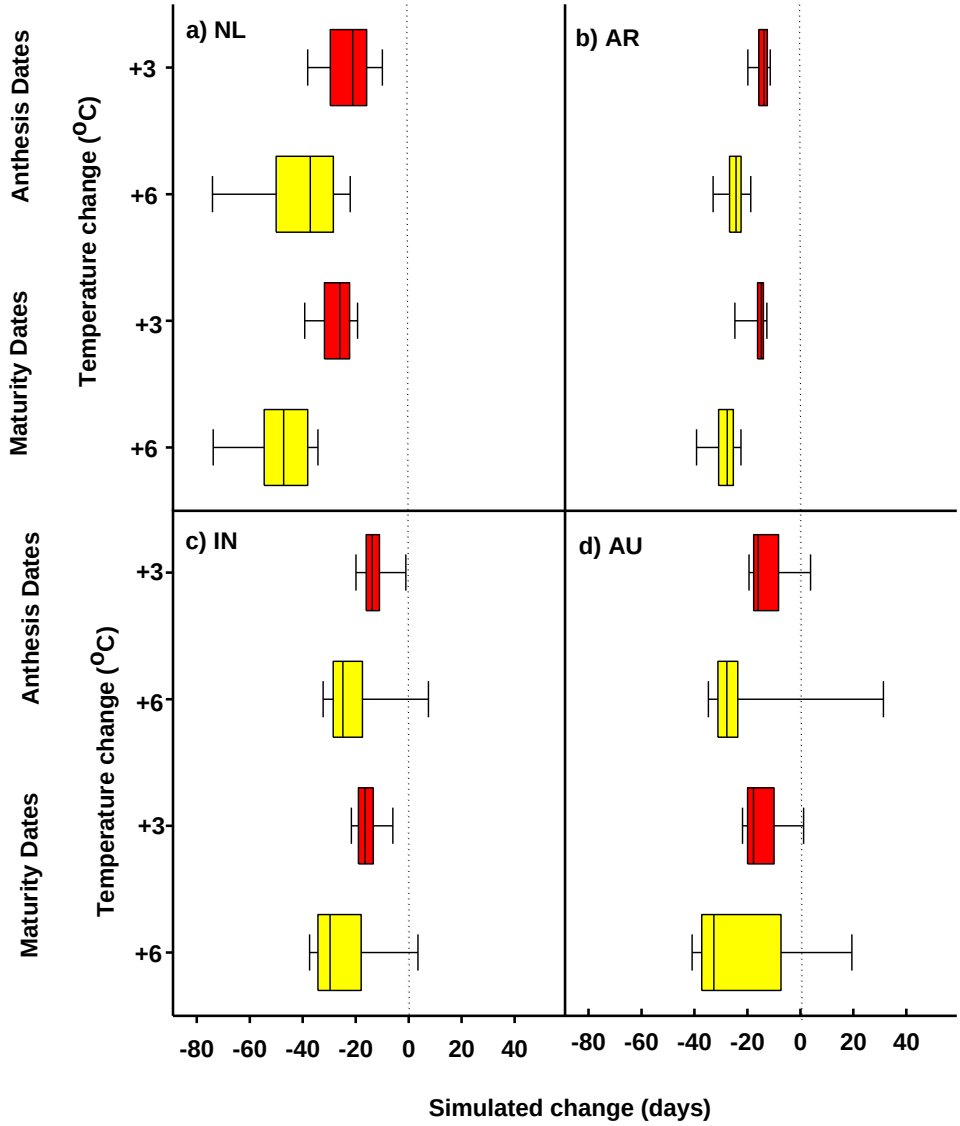

Supplementary Fig. S3. Simulated changes in anthesis and maturity dates with increased temperatures of +3°C (red) and +6°C (yellow). For each box plot, vertical lines represent, from left to right, the 10th percentile, 25th percentile, median, 75th percentile and 90th percentile of simulations based on multi-models.

The scenario with seven consecutive days of T_{max} of 35 ^{o}C at the mean anthesis date for each location is one of the special simulation experiments (Supplementary Table S5). The impact of this scenario is shown in Supplementary Fig. S4, indicating that some of the increased variation with increasing temperature in Fig. 3 is due to the contribution of variation in modeling heat stress impact on yields (Supplementary Fig. S4).

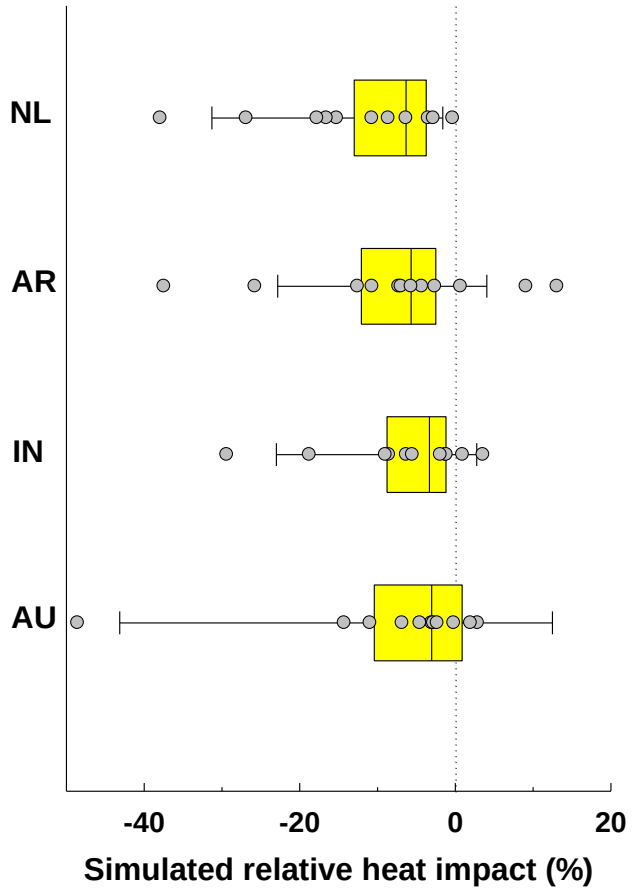

Supplementary Fig. S4. Simulated yield change from seven days of introduced T_{max} of 35 ^{o}C at the mean anthesis date for each location. For each box plot, vertical lines represent, from left to right, the 10th percentile, 25th percentile, median, 75th percentile and 90th percentile of simulations based on multi-models. Symbols indicate results from models which account for heat stress impact (see Supplementary Table S2, column 9)

Temperature by CO_2 impact

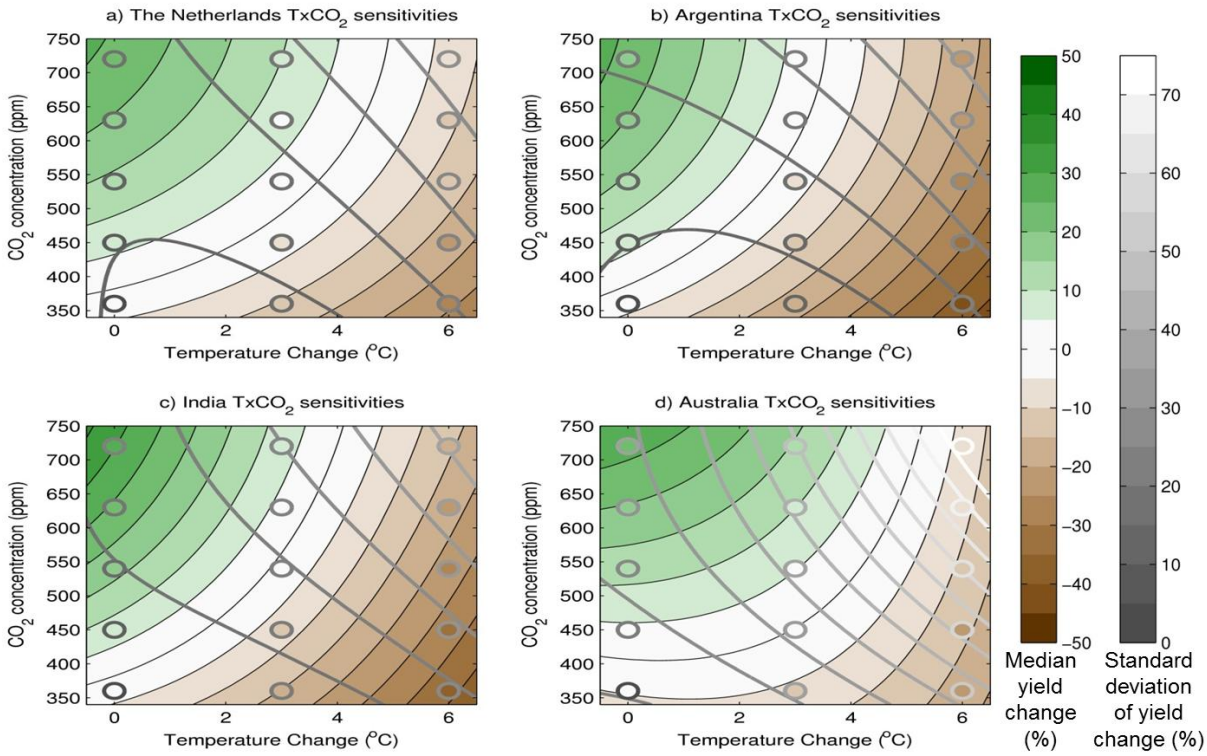

Supplementary Fig. S5: Response surfaces of crop model ensemble to temperature and atmospheric CO_2 concentration sensitivity tests at *a)* the Netherlands, *b)* Argentina, *c)* India, and *d)* Australia. The filled colours represent the median (across the 26 crop models) 30-year mean yield change (as a percentage of the mean 30-year yield for the 1981-2010 baseline period) for each of the sensitivity experiments (dots) as well as an emulated surface fit to these dots. The gray colours represent the standard deviation (across the 26 crop models) of the 30-year mean yield change (percentage of the 30-year mean baseline yield), with the outlines of the dots representing the experiments and the contours representing an emulated surface fit to these experimental standard deviations.

Response emulators for median yield change and the standard deviation of yield change (across the 26 crop models) were fit assuming a quadratic form (Supplementary Fig. S5):

$$E(T,[CO_2]) = a + bT + cT^2 + d[CO_2] + e[CO_2]^2 + fT[CO_2] + g\,(T[CO2])^2$$

where $E(T,CO_2)$ is the emulated response at a given temperature change T and CO_2 concentration ($[CO_2]$) and parameters *a-g* are fit using a least-squares fit.

The results indicate that the general pattern of yield sensitivities and their uncertainties is consistent from region to region, although the magnitude of the sensitivities varies from site to site. Yields tend to be decreased at higher temperature and increased at higher CO_2 concentration; however, at high temperatures the CO_2 benefits are reduced (Supplementary Fig. S5). As the ensemble of crop models is tested with climates that are increasingly dissimilar from the baseline period (e.g. very hot and with high CO_2), uncertainty also increases. This effect is strongest in Australia (where the baseline climate is hot and dry) and weakest in The Netherlands (where the baseline climate is cool and wet).

Supplementary References

1. Groot, J.J.R. & Verberne, E.L.J. in Nitrogen Turnover in the Soil-Crop System. Modelling of Biological Transformations, Transport of Nitrogen and Nitrogen Use Efficiency. Proceedings of a Workshop (eds. Groot, J.J.R., De Willigen, P. & Verberne, E.L.J.) 349-383 (Institute for Soil Fertility Research, Haren, The Netherlands, 1991).
2. Travasso, M.I., Magrin, G.O., Rodríguez, R. & Grondona, M.O. Comparing CERES-wheat and SUCROS2 in the Argentinean Cereal Region. *MODSIM 1995 International Congress on Modelling and Simulation*, 366-369 (1995).
3. Naveen, N. Evaluation of soil water status, plant growth and canopy environment in relation to variable water supply to wheat (IARI, New Delhi., 1986).
4. Asseng, S. et al. Performance of the APSIM-wheat model in Western Australia. *Field Crops Research* **57**, 163-179 (1998).
5. Asseng, S. et al. Simulated wheat growth affected by rising temperature, increased water deficit and elevated atmospheric CO2. *Field Crops Research* **85**, 85-102 (2004).
6. Keating, B.A. et al. An overview of APSIM, a model designed for farming systems simulation. *European Journal of Agronomy* **18**, 267-288 (2003).
7. Steduto, P., Hsiao, T., Raes, D. & Fereres, E. AquaCrop-The FAO Crop Model to Simulate Yield Response to Water: I. Concepts and Underlying Principles. *Agronomy Journal* **101**, 426-437 (2009).
8. Stockle, C., Donatelli, M. & Nelson, R. CropSyst, a cropping systems simulation model. *European Journal of Agronomy* **18**, 289-307 (2003).
9. Hoogenboom, G. & White, J. Improving physiological assumptions of simulation models by using gene-based approaches. *Agronomy Journal* **95**, 82-89 (2003).

10. Jones, J. et al. The DSSAT cropping system model. *European Journal of Agronomy* **18**, 235-265 (2003).
11. Ritchie, J.T., Godwin, D.C. & Otter-Nacke, S. CERES-wheat: A user-oriented wheat yield model. Preliminary documentation (1985).
12. Hunt, L.A. & Pararajasingham, S. CROPSIM-wheat - a model describing the growth and development of wheat. *Canadian Journal of Plant Science* **75**, 619-632 (1995).
13. Grant, R. et al. Controlled Warming Effects on Wheat Growth and Yield: Field Measurements and Modeling. *Agronomy Journal* **103**, 1742-1754 (2011).
14. Kiniry, J. et al. EPIC model parameters for cereal, oilseed, and forage crops in the northern great-plains region. *Canadian Journal of Plant Science* **75**, 679-688 (1995).
15. Williams, J., Jones, C., Kiniry, J. & Spanel, D. The EPIC crop growth-model. *Transactions of the ASAE* **32**, 497-511 (1989).
16. Izaurralde, R.C., McGill, W.B. & Williams, J.R. in Managing agricultural greenhouse gases: Coordinated agricultural research through GRACEnet to address our changing climate (eds. Liebig, M.A., Franzluebbers, A.J. & Follett, R.F.) 409-429 (Elsevier, Amsterdam, 2012).
17. Priesack, E., Gayler, S. & Hartmann, H. The impact of crop growth sub-model choice on simulated water and nitrogen balances. *Nutrient Cycling in Agroecosystems* **75**, 1-13 (2006).
18. Ritchie, S., Nguyen, H. & Holaday, A. Genetic diversity in photosynthesis and water-use efficiency of wheat and wheat relatives. *Journal of Cellular Biochemistry*, 43-43 (1987).
19. Biernath, C. et al. Evaluating the ability of four crop models to predict different environmental impacts on spring wheat grown in open-top chambers. *European Journal of Agronomy* **35**, 71-82 (2011).
20. Stenger, R., Priesack, E., Barkle, G. & Sperr, C. (Land Treatment collective proceedings Technical Session, New Zealand, 1999).
21. Wang, E. & Engel, T. SPASS: a generic process-oriented crop model with versatile windows interfaces. *Environmental Modelling & Software* **15**, 179-188 (2000).
22. Yin, X. & van Laar, H.H. Crop systems dynamics: an ecophysiological simulation model of genotype-by-environment interactions (Wageningen Academic Publishers, Wageningen, The Netherlands, 2005).
23. Goudriaan, J. & Van Laar, H.H. (eds.) Modelling Potential Crop Growth Processes. Textbook With Exercises (Kluwer Academic Publishers, Dordrecht, The Netherlands, 1994).
24. Berntsen, J., Petersen, B.M., Jacobsen, B., Olesen, J.E. & Hutchings, N.J. Evaluating nitrogen taxation scenarios using the dynamic whole farm simulation model FASSET. *Agricultural Systems* **76**, 817-839 (2003).
25. Olesen, J.E. et al. Comparison of methods for simulating effects of nitrogen on green area index and dry matter growth in winter wheat. *Field Crops Research* **74**, 131-149 (2002).
26. Challinor, A., Wheeler, T., Craufurd, P., Slingo, J. & Grimes, D. Design and optimisation of a large-area process-based model for annual crops. *Agricultural and Forest Meteorology* **124**, 99-120 (2004).
27. Li, S. et al. Simulating the Impacts of Global Warming on Wheat in China Using a Large Area Crop Model. *Acta Meteorologica Sinica* **24**, 123-135 (2010).
28. Kersebaum, K. Modelling nitrogen dynamics in soil-crop systems with HERMES. *Nutrient Cycling in Agroecosystems* **77**, 39-52 (2007).
29. Kersebaum, K.C. Special features of the HERMES model and additional procedures for parameterization, calibration, validation, and applications. *Ahuja, L.R. and Ma, L. (eds.). Methods of introducing system models into agricultural research. Advances in Agricultural Systems Modeling Series 2, Madison (ASA-CSSA-SSSA)*, 65-94 (2011).

30. Aggarwal, P. et al. InfoCrop: A dynamic simulation model for the assessment of crop yields, losses due to pests, and environmental impact of agro-ecosystems in tropical environments. II. Performance of the model. *Agricultural Systems* **89**, 47-67 (2006).
31. Spitters, C.J.T. & Schapendonk, A.H.C.M. Evaluation of breeding strategies for drought tolerance in potato by means of crop growth simulation. *Plant and Soil* **123**, 193-203 (1990).
32. Shibu, M., Leffelaar, P., van Keulen, H. & Aggarwal, P. LINTUL3, a simulation model for nitrogen-limited situations: Application to rice. *European Journal of Agronomy* **32**, 255-271 (2010).
33. Angulo, C. et al. Implication of crop model calibration strategies for assessing regional impacts of climate change in Europe. *Agricultural and Forest Meteorology* **170**, 32-46 (2013).
34. Bondeau, A. et al. Modelling the role of agriculture for the 20th century global terrestrial carbon balance. *Global Change Biology* **13**, 679-706 (2007).
35. Beringer, T., Lucht, W. & Schaphoff, S. Bioenergy production potential of global biomass plantations under environmental and agricultural constraints. *Global Change Biology Bioenergy* **3**, 299-312 (2011).
36. Fader, M., Rost, S., Muller, C., Bondeau, A. & Gerten, D. Virtual water content of temperate cereals and maize: Present and potential future patterns. *Journal of Hydrology* **384**, 218-231 (2010).
37. Gerten, D., Schaphoff, S., Haberlandt, U., Lucht, W. & Sitch, S. Terrestrial vegetation and water balance - hydrological evaluation of a dynamic global vegetation model. *Journal of Hydrology* **286**, 249-270 (2004).
38. Rost, S. et al. Agricultural green and blue water consumption and its influence on the global water system. *Water Resources Research* **44** (2008).
39. Müller, C. et al. Effects of changes in CO2, climate, and land use on the carbon balance of the land biosphere during the 21st century. *Journal of Geophysical Research-Biogeosciences* **112** (2007).
40. Tao, F., Yokozawa, M. & Zhang, Z. Modelling the impacts of weather and climate variability on crop productivity over a large area: A new process-based model development, optimization, and uncertainties analysis. *Agricultural and Forest Meteorology* **149**, 831-850 (2009).
41. Tao, F., Zhang, Z., Liu, J. & Yokozawa, M. Modelling the impacts of weather and climate variability on crop productivity over a large area: A new super-ensemble-based probabilistic projection. *Agricultural and Forest Meteorology* **149**, 1266-1278 (2009).
42. Tao, F. & Zhang, Z. Adaptation of maize production to climate change in North China Plain: Quantify the relative contributions of adaptation options. *European Journal of Agronomy* **33**, 103-116 (2010).
43. Tao, F. & Zhang, Z. Climate change, wheat productivity and water use in the North China Plain: A new super-ensemble-based probabilistic projection. *Agricultural and Forest Meteorology ISSN 0168-1923,* (2011).
44. Nendel, C. et al. The MONICA model: Testing predictability for crop growth, soil moisture and nitrogen dynamics. *Ecological Modelling* **222**, 1614-1625 (2011).
45. Oleary, G., Connor, D. & White, D. A simulation-model of the development, growth and yield of the wheat crop. *Agricultural Systems* **17**, 1-26 (1985).
46. OLeary, G. & Connor, D. A simulation model of the wheat crop in response to water and nitrogen supply .1. Model construction. *Agricultural Systems* **52**, 1-29 (1996).
47. OLeary, G. & Connor, D. A simulation model of the wheat crop in response to water and nitrogen supply .2. Model validation. *Agricultural Systems* **52**, 31-55 (1996).
48. Latta, J. & O'Leary, G. Long-term comparison of rotation and fallow tillage systems of wheat in Australia. *Field Crops Research* **83**, 173-190 (2003).

49. Basso, B., Cammarano, D., Troccoli, A., Chen, D. & Ritchie, J. Long-term wheat response to nitrogen in a rainfed Mediterranean environment: Field data and simulation analysis. *European Journal of Agronomy* **33**, 132-138 (2010).
50. Senthilkumar, K. et al. Characterising rice-based farming systems to identify opportunities for adopting water efficient cultivation methods in Tamil Nadu, India. *Agricultural Water Management* **96**, 1851-1860 (2009).
51. Jamieson, P., Semenov, M., Brooking, I. & Francis, G. Sirius: a mechanistic model of wheat response to environmental variation. *European Journal of Agronomy* **8**, 161-179 (1998).
52. Jamieson, P. & Semenov, M. Modelling nitrogen uptake and redistribution in wheat. *Field Crops Research* **68**, 21-29 (2000).
53. Lawless, C., Semenov, M. & Jamieson, P. A wheat canopy model linking leaf area and phenology. *European Journal of Agronomy* **22**, 19-32 (2005).
54. Semenov, M. & Shewry, P. Modelling predicts that heat stress, not drought, will increase vulnerability of wheat in Europe. *Scientific Reports* **1** (2011).
55. Martre, P. et al. Modelling protein content and composition in relation to crop nitrogen dynamics for wheat. *European Journal of Agronomy* **25**, 138-154 (2006).
56. Ferrise, R., Triossi, A., Stratonovitch, P., Bindi, M. & Martre, P. Sowing date and nitrogen fertilisation effects on dry matter and nitrogen dynamics for durum wheat: An experimental and simulation study. *Field Crops Research* **117**, 245-257 (2010).
57. He, J., Stratonovitch, P., Allard, V., Semenov, M.A. & Martre, P. Global Sensitivity Analysis of the Process-Based Wheat Simulation Model SiriusQuality1 Identifies Key Genotypic Parameters and Unravels Parameters Interactions. *Procedia - Social and Behavioral Sciences* **2**, 7676-7677 (2010).
58. Brisson, N. et al. STICS: a generic model for the simulation of crops and their water and nitrogen balances. I. Theory and parameterization applied to wheat and corn. *Agronomie* **18**, 311-346 (1998).
59. Brisson, N. et al. An overview of the crop model STICS. *European Journal of Agronomy* **18**, 309-332 (2003).
60. Boogaard, H.L., Van Diepen, C.A., Rötter, R.P., Cabrera, J.C.M.A., Van Laar, H.H. User's guide for the OFOST 7.1 crop growth simulation model and WOFOST control center 1.5. Technical Document 52, Winand Staring Centre, Wageningen, The Netherlands, 144pp. (1998)
61. Hoogenboom, G. et al. (University of Hawaii, Honolulu, Hawaii, 2010).
62. Bosilovich, M.G., Robertson, F.R. & Chen, J. Global Energy and Water Budgets in MERRA. *Journal of Climate* **24**, 5721-5739 (2011).
63. Palosuo, T. et al. Simulation of winter wheat yield and its variability in different climates of Europe: A comparison of eight crop growth models. *European Journal of Agronomy* **35**, 103-114 (2011).
64. Taylor, S.L., Payton, M.E. & Raun, W.R. Relationship between mean yield, coefficient of variation, mean square error, and plot size in wheat field experiments. *Communications in Soil Science and Plant Analysis* **30**, 1439-1447 (1999).
65. Bert, F.E., Laciana, C.E., Podestá, G.P., Satorre, E.H. & Menéndez, A.N. Sensitivity of CERES-Maize simulated yields to uncertainty in soil properties and daily solar radiation. *Agricultural Systems* **94**, 141-150 (2007).
66. Št'astná, M. & Žalud, Z. Sensitivity analysis of soil hydrologic parameters for two crop growth simulation models. *Soil and Tillage Research* **50**, 305-318 (1999).
67. Amthor, J.S. Effects of atmospheric CO2 concentration on wheat yield: review of results from experiments using various approaches to control CO2 concentration. *Field Crops Research* **73**, 1-34 (2001).

68. Ewert, F. et al. Effects of elevated CO2 and drought on wheat: testing crop simulation models for different experimental and climatic conditions. *Agriculture Ecosystems & Environment* **93**, 249-266 (2002).
69. Li, W., Han, X., Zhang, Y. & Li, Z. Effects of elevated CO2 concentration, irrigation and nitrogenous fertilizer application on the growth and yield of spring wheat in semi-arid areas. *Agricultural Water Management* **87**, 106-114 (2007).
70. Hogy, P., Keck, M., Niehaus, K., Franzaring, J. & Fangmeier, A. Effects of atmospheric CO(2) enrichment on biomass, yield and low molecular weight metabolites in wheat grain. *Journal of Cereal Science* **52**, 215-220 (2010).
71. Ko, J. et al. Simulation of free air CO(2) enriched wheat growth and interactions with water, nitrogen, and temperature. *Agricultural and Forest Meteorology* **150**, 1331-1346 (2010).
72. Kimball, B.A. in Handbook of Climate Change and Agroecosystems – Impacts, Adaptation, and Mitigation, Hillel, D., and Rosenzweig, C. (Eds). (Imperial College Press, London, 2011).
73. Xiao, G., Liu, W., Xu, Q., Sun, Z. & Wang, J. Effects of temperature increase and elevated CO2 concentration, with supplemental irrigation, on the yield of rain-fed spring wheat in a semiarid region of China. *Agricultural Water Management* **74**, 243-255 (2005).
74. Kristensen, K., Schelde, K. & Olesen, J.E. Winter wheat yield response to climate variability in Denmark. *Journal of Agricultural Science* **149** (2011).
75. Wilby, R.L. et al. A review of climate risk information for adaptation and development planning. *International Journal of Climatology* **29**, 1193-1215 (2009).
76. Randall, D.A. et al. in Climate Change 2007: The Physical Science Basis. Contribution of Working Group I to the Fourth Assessment Report of the Intergovernmental Panel on Climate Change (eds. Solomon, S. et al.) 589-662 (Cambridge University Press, Press, Cambridge, UK, 2007).